REPORT DOCUMENTATION PAGE

Form Approved
OMB No. 0704-0188

1. REPORT DATE *(DD-MM-YYYY)*	2. REPORT TYPE	3. DATES COVERED *(From - To)*
03-31-2009	Final Technical Report	11/01/2005 - 12/31/2008

4. TITLE AND SUBTITLE
Advanced Underwater Imaging: Final Technical Report

5a. CONTRACT NUMBER

5b. GRANT NUMBER
N000140610113

5c. PROGRAM ELEMENT NUMBER

6. AUTHOR(S)
Fraser R. Dalgleish, Ph.D
Frank M. Caimi, Ph.D
Walter B. Britton

5d. PROJECT NUMBER

5e. TASK NUMBER

5f. WORK UNIT NUMBER

7. PERFORMING ORGANIZATION NAME(S) AND ADDRESS(ES)
Harbor Branch Oceanographic Institute at Florida Atlantic University
5600 US 1 North, Fort Pierce, FL 34946

8. PERFORMING ORGANIZATION REPORT NUMBER

9. SPONSORING/MONITORING AGENCY NAME(S) AND ADDRESS(ES)
Office of Naval Research
875 North Randolph St.
Arlington, VA 22203-1995

10. SPONSOR/MONITOR'S ACRONYM(S)
ONR

11. SPONSOR/MONITOR'S REPORT NUMBER(S)

12. DISTRIBUTION/AVAILABILITY STATEMENT
Approved for Public Release

13. SUPPLEMENTARY NOTES

14. ABSTRACT

The long-term goal of this research is to advance the knowledge necessary to develop wide-swath laser-based underwater imaging systems that provide greater sensitivity over longer ranges than existing systems. In addition, since existing imaging systems are physically incompatible with small form-factor Autonomous Underwater Vehicles (AUVs), this effort concentrated on methods specifically aimed at size reduction while improving or maintaining image performance. The primary application for these systems is in imaging both natural and man-made objects in aquatic environments.

15. SUBJECT TERMS

16. SECURITY CLASSIFICATION OF:			17. LIMITATION OF ABSTRACT	18. NUMBER OF PAGES	19a. NAME OF RESPONSIBLE PERSON
a. REPORT	b. ABSTRACT	c. THIS PAGE			19b. TELEPHONE NUMBER *(Include area code)*

Advanced Underwater Imaging: Final Technical Report

Award Period: 11/01/2005 – 12/31/2008
Grant Number: N000140610113

Harbor Branch Oceanographic Institute at Florida Atlantic University
5600 US 1 North, Ft. Pierce, FL 34946
Phone: (772) 465 2400 extn: 591
E-mail: fdalglei@hboi.fau.edu

LONG-TERM GOALS

The long-term goal of this research is to advance the knowledge necessary to develop wide-swath laser-based underwater imaging systems that provide greater sensitivity over longer ranges than existing systems. In addition, since existing imaging systems are physically incompatible with small form-factor Autonomous Underwater Vehicles (AUVs), this effort concentrated on methods specifically aimed at size reduction while improving or maintaining image performance. The primary application for these systems is in imaging both natural and man-made objects in aquatic environments.

OBJECTIVES

The objectives of the work performed during the duration of this grant were to:

1) Develop time history and imaging simulation tools for investigation of pulsed-laser techniques to reduce image noise resulting from scattered light and/or background natural illumination.
2) Gain an understanding of the validity and limitations of the simulations using benchtop hardware systems, by comparing simulation results with measured data.
3) Gain an understanding of the technological and system performance trade-offs in the design of wide-swath pulsed-gated optical imagers which are suitable to be deployed from a small form factor AUV.
4) Analyze the performance of candidate autonomous image quality optimization computer algorithms using measured data and provide image quality metrics for comparison of the pulsed-gated and continuous wave (CW) extended range laser imaging methods.
5) Investigate the potential to achieve increased system range and image contrast via the use of high frequency pulse modulation and coding techniques.

APPROACH

In April and June 2005 two meetings were held with members of the laser line scan (LLS) user community to discuss user requirements and possible technical approaches for meeting these requirements. Emphasis was placed on approaches that could lead to a new system design in the relatively short term.

Following these meetings, several projects were initiated under the Advanced Underwater Imaging (AUI) program:

1. A project to develop suitable pulsed laser technology (PSI and Q-Peak)
2. The design of a compact LLS imaging system to allow for side-by-side benchtop comparisons of pulsed and CW imaging system alternatives (HBOI and Lincoln Laser)
3. The development of a dedicated extended range underwater laser imaging test facility (HBOI)
4. The development of radiative transfer models which would allow accurate side-by-side comparison of system concepts (Metron and PSI)

The approach developed throughout the three year funding period involved continuing collaborations with Metron Inc (Reston, VA) and Physical Sciences Inc (Andover, MA). Metron was responsible for developing and refining radiative transfer simulation tools as part of their EODES suite, and in analyzing test-tank data and images versus simulated data and images. PSI was tasked with performing simulations with the radiative transfer code to identify the potential benefits of the use of pulsed-gated LLS architectures; performing analysis of experimental data in the validation of the pulse time history code; developing image analysis algorithms for comparing alternate LLS configurations.

In summary, the proposed technical approach during the three year award period consisted of the following activities:

1. Development and enhancement of pulsed-gated radiative transfer code to simulate pulse time history and image simulations for the pulsed-gated LLS.
2. Development and fabrication of a benchtop LLS scan architecture and configuration with sources and receivers necessary to compare both CW-LLS and Pulsed-gated LLS (PG-LLS) under identical operational conditions for the purpose of determining the relative advantages of the pulsed-gated approach.
3. Rigorous test-tank validation of laser pulse time history radiative transfer model, including experimental measurement of beam spread function over extended distances.
4. Development and application of image quality algorithms as comparative performance metrics for images acquired.
5. Experimental and analytic comparison between CW-LLS and PG-LLS imagers using performance metrics.
6. More advanced simulations and experimental validation for alternate laser sources, such as short pulse modulated lasers.

WORK COMPLETED AND SIGNIFICANT RESULTS

1. Experimental validation of laser pulse time history code

A series of experiments was conducted with the Q-Peak pulsed laser in the HBOI imaging test facility to validate the performance of the Metron radiative transfer time history model. Scattering was varied by the addition of Maalox and optical properties were measured with a Wetlabs ac-9 meter. Parameters such as receiver aperture, source-receiver separation (SR), the pointing angle of the receiver and the turbidity of the water were systematically varied and a series of pulse time histories were recorded at a 5 GHz sampling rate for each set of conditions. The measured and modeled results were then

compared. Discrepancies were evaluated to determine if the issue lay with the model or with the experiment. A set of results is shown in figure 1.

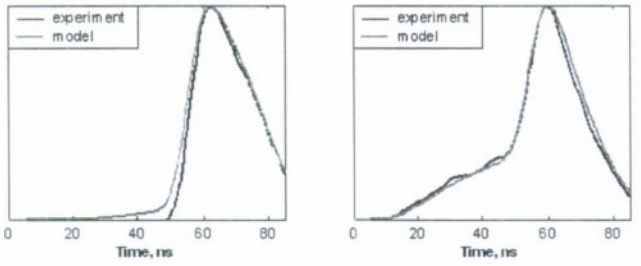

Graphs of the experimental data (red) and model results (green). Left: c=0.08 m^{-1}, SR=376mm, aperture = 3mm. Right: c=0.25 m^{-1}, SR=376mm, aperture = 3mm.

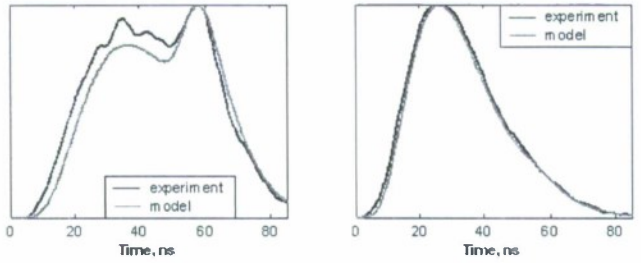

Graphs of the experimental data (red) and model results (green). Left: c=0.48 m^{-1}, SR=376mm, aperture = 3mm. Right: c=0.63 m^{-1}, SR=376mm, aperture = 3mm.

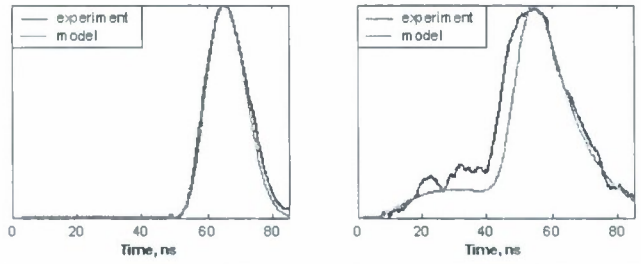

Graphs of the experimental data (red) and model results (green). Left: c=0.06 m^{-1}, SR=250mm, aperture = 1mm. Right: c=0.25 m^{-1}, SR=83mm, aperture = 1mm.

Figure 1: A selection of results from the experimental validation of the Metron underwater laser pulse time history simulation software.

The model has proven to be a good predictor of pulse behavior, and the validation effort supports its use as a design tool for the development of the PG-LLS imaging system.

2. Application of Image Quality algorithms to acquired images.

The acquired images were analyzed using a variety of image quality metrics to compare the relative contrast and signal-to-noise ratios versus attenuation coefficient and stand-off distance. Image quality metrics for two applications of image analysis were investigated: optimizing image quality in the field during image acquisition by an autonomous system, and comparing images of test targets obtained in the HBOI imaging facility. In the field the challenge is ensuring that an imaging system is acquiring

the best possible images under the operating conditions that exist at the time, which might require adjusting system configuration parameters, while in the laboratory the need is to evaluate the impacts of controlled changes in experimental parameters, or to compare the performance of alternative imaging configurations. For the field application, approaches were investigated that are used for autofocus in digital cameras. These systems vary the lens position, compute a sharpness metric from the image at each position, and then set the lens at the best position according to the metric. The analogy for a laser imaging system in the field, is that parameters such as alignment angle could be varied, and the images compared in a similar manner. Based on the results reported in Shih (2007), which compared a wide variety of autofocus metrics in a systematic way, we selected the Tenengrad-Sobel (T-S) metric for further experimentation. The Tenengrad/Sobel algorithm adopts a 2D spatial gradient measurement approach for sharpness determination. A typical operator uses a 3x3 or larger matrix to detect edges in the horizontal and vertical directions. For each image pixel, the algorithm derives two fitness values based on the horizontal (G_x) and vertical neighbors (G_y), and these are then used collectively to determine the overall fitness value. Intuitively, these fitness values represent the gradient magnitudes at each point in the image. For example:

$$G_x = \begin{matrix} -1 & 0 & 1 \\ -2 & 0 & 2 \\ -1 & 0 & 1 \end{matrix} \qquad G_y = \begin{matrix} 1 & 2 & 1 \\ 0 & 0 & 0 \\ -1 & -2 & -1 \end{matrix}$$

The overall fitness function is then given (for an M x N matrix) by:

$$F(i,j) = \sum_{i=1}^{M} \sum_{j=1}^{N} \sqrt{G_x(i,j)^2 + G_y(i,j)^2} \qquad \text{Equation 1}$$

For laboratory work we applied the T-S algorithm, but in addition applied several contrast and signal to noise algorithms for the technical target work, specifically a conventional contrast ratio and the contrast signal-to-noise ratio:

Contrast ratio: $$\frac{WhiteMean - BlackMean}{WhiteMean + BlackMean} \qquad \text{Equation 2}$$

Contrast SN ratio: $$\frac{WhiteMean - BlackMean}{\sqrt{WhiteSTD^2 + BlackSTD^2}} \qquad \text{Equation 3}$$

The contrast ratios were computed for raw target images with means and standard deviations computed over adjacent 'black' and 'white' areas of the technical target. The computed values help in comparing images both between and within system types.

In order to test the T-S autofocus approach using the HBOI test facility we acquired images of artificial targets with 'ideal' settings and with intentional image degradation induced by misaligning the receiver. Figure 2 shows the master image collected and a target sub-image selected therefrom.

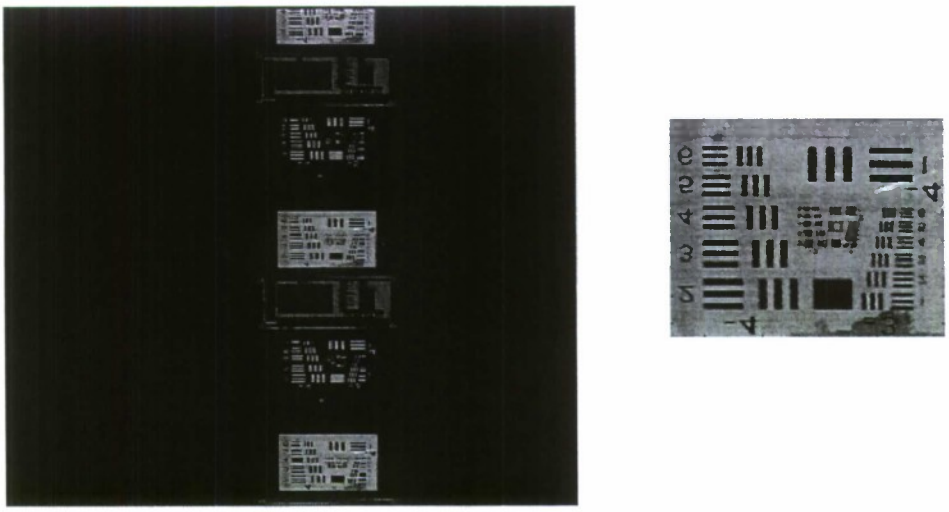

Figure 2: Master image (left) and selected target image.

The fitness value computed by the T-S algorithm was nearly identical for the two images of each target selected from the master image, but different from one target to another, showing that the absolute value of the metric is dependent on image content. The fitness values computed from different master images for a given target followed the desired trend – the fitness value decreased as the receiver misalignment increased. The trend matched subjective judgment of relative image quality among the images. An approach of this sort could be applied in the field by varying system parameters on the fly. Because of platform movement the T-S algorithm would be applied to different images, but if the bottom type is relatively consistent at a textural level the images and results could be treated as pseudo-static. The benefit of this approach would be realized in systems in which human operator adjustment is not desired or possible.

3. Test-tank imager comparison between PG-LLS and CW-LLS

A series of experiments was conducted using the benchtop laser line scanner (source/receiver separation = 23.4cm) in the imaging test facility at realistic stand-off distances in a variety of turbidity conditions ranging from very clear conditions to greater than 7 attenuation lengths. Scattering was varied by the addition of Maalox and optical properties were measured with the ac-9 meter. The full set of image data at the various turbidities were first made with the CW-LLS configuration. The water in the tank was then filtered for several days to insure clarity, measurements were verified with the ac-9 meter, and the PG-LLS components were installed. Correct alignment was verified, and the turbidity cycling and image acquisition sequence was repeated. System parameters were adjusted to allow for a fair comparison.

To illustrate the effect that gating out the backscatter component has on target contrast as a function of beam attenuation lengths, the contrast (equation 2) of both the white-on-black (WoB) and black-on-white (BoW) target images were computed for both imaging methods. Furthermore, to investigate the effect that increased forward scatter has on image contrast, two different receiver angular apertures were used for both imaging methods for both targets. The BoW contrast is shown in Figure 3. Although all four cases exhibit similar clear water contrast, it can be seen that the narrow receiver

angle (15mrad) CW-LLS images have superior contrast compared to the wider receiver angle (30mrad) PG-LLS configuration until approximately 5 attenuation lengths, thus suggesting that the contrast reduction due to multiple backscatter dominates the contrast reduction due to forward scatter for the non-gated system images at beyond 5 attenuation lengths. The narrow receiver angle PG-LLS case, which removes almost all backscatter and significantly reduces forward scatter, produced superior contrast throughout the entire experiment.

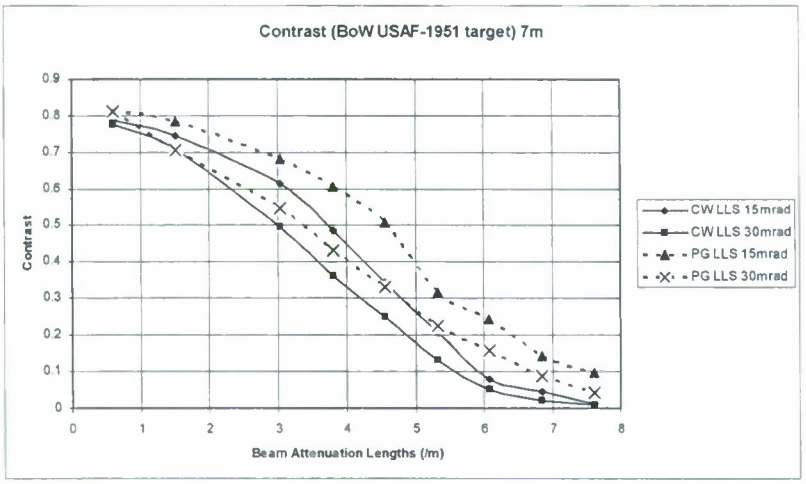

Figure 3: Computed contrast for USAF-1951 Black-on-White target at 7m for CW-LLS versus PG-LLS

Considering the WoB results of figure 4, it is clear that the lower background reflectance results in a lower forward scatter signal, and the PG-LLS with the wider aperture has a consequent superior contrast compared to the narrower aperture CW-LLS for 3.5 attenuation lengths and beyond.

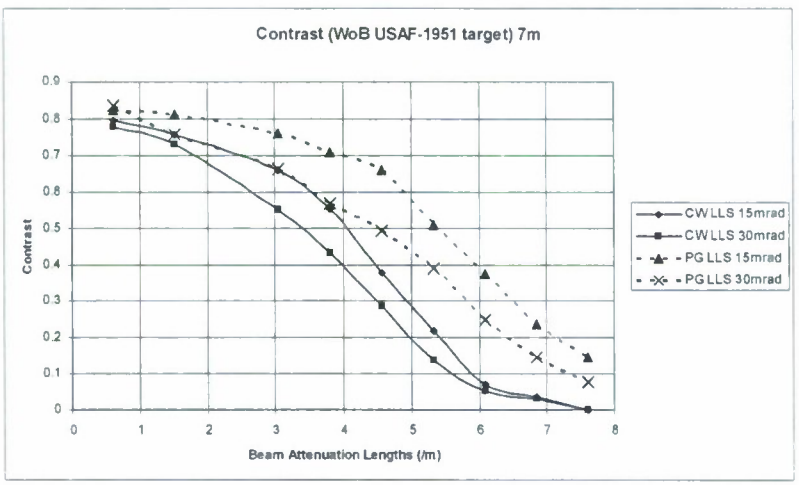

Figure 4: Computed contrast for USAF-1951 White-on-Black target at 7m for CW-LLS versus PG-LLS

As expected from simulations, the CW-LLS image contrast (equation 2) becomes backscatter limited in turbid water (i.e. since the backscatter can not be removed, it eventually dominates and masks the useful image content). At 7.6 beam attenuation lengths, the PG-LLS images becomes contrast limited only due to forward scatter when the target background reflectance is high, since the backscatter is substantially reduced by gating, leaving only the forward scatter signal from adjacent regions of the target to limit the contrast. On the other hand, the PG-LLS images with the low reflectance target background had a higher contrast in the 7.6 beam attenuation lengths case, and might be considered approaching power (or photon) limit. In this latter case, the contrast could be improved with increasing laser pulse energy, whereas for the high reflectance background case the PG-LLS would reach a contrast limit due to forward scatter. Note that for both the CW-LLS and PG-LLS images the BoW target has a lower contrast than the WoB target. This results from the forward scatter degrading the contrast in both cases. This effect can also be seen in the captured images. Figure 5 shows the image sequence for the BoW target clearly resulting in the contrast limited case for both the CW-LLS (left hand columns) and PG-LLS (right hand columns) cases, occurring earlier for the wider aperture cases. Figure 6 shows the WoB image sequences, where the limiting cases clearly show the difference between a contrast limited and a power (or photon) limited regime.

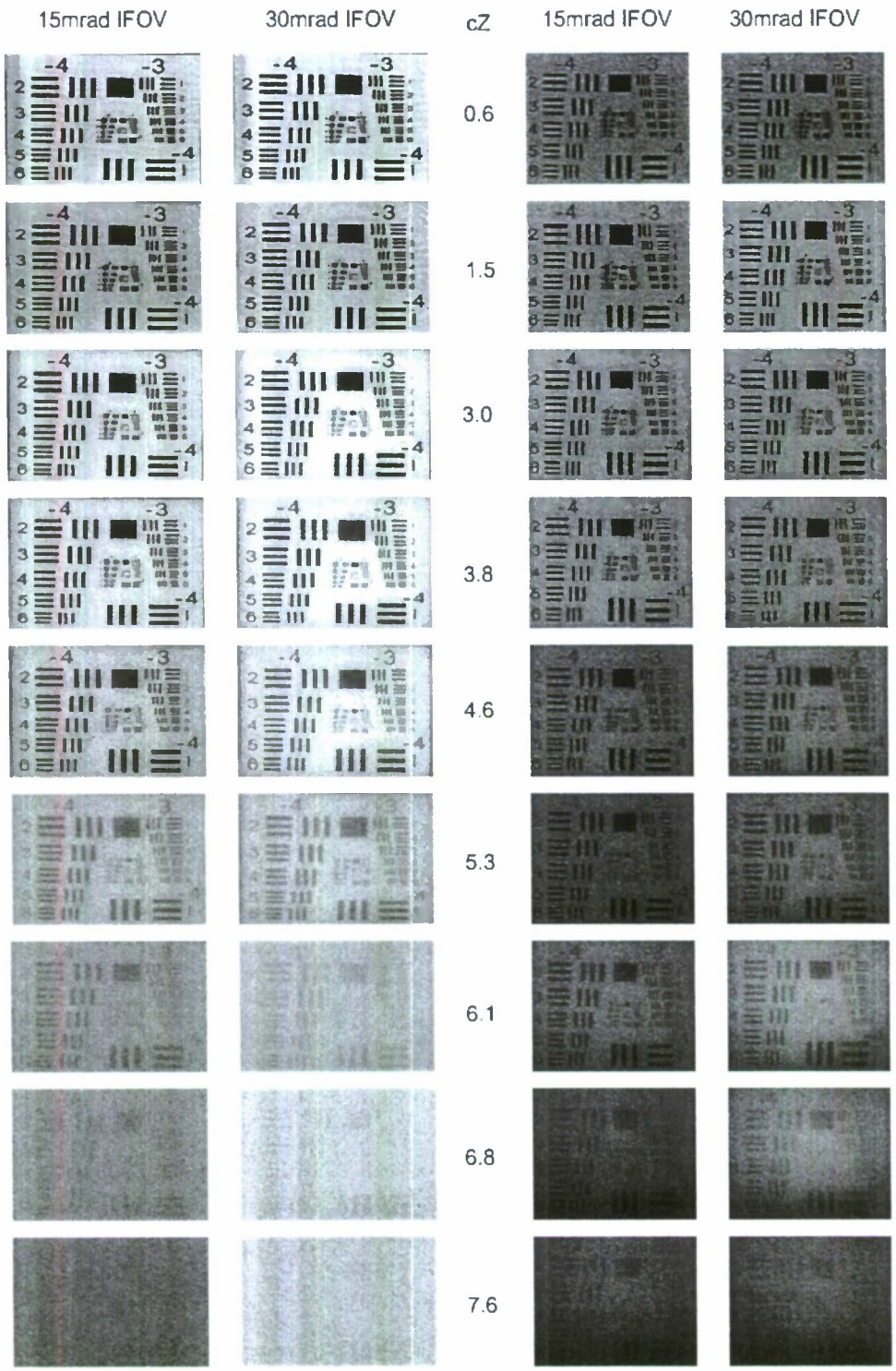

Figure 5: Image sequences from the CW-LLS (left hand columns) and PG-LLS (right hand columns) imagers with the USAF-1951 black-on-white target. Receiver angular aperture (in milliradians) and cZ, the number of attenuation lengths is also shown.

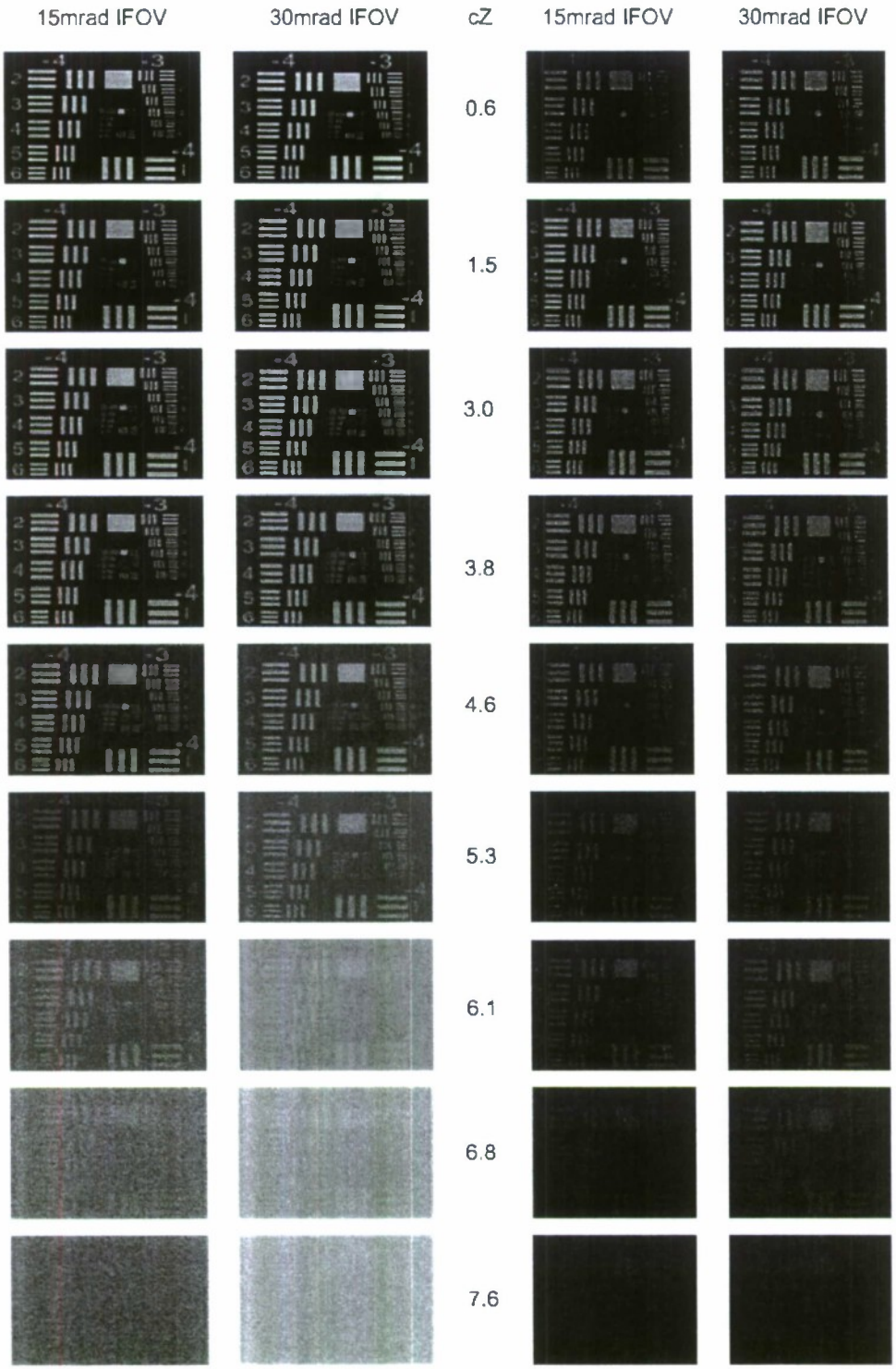

Figure 6: Image sequences from the CW-LLS (left hand columns) and PG-LLS (right hand columns) imagers with the USAF-1951 white-on-black target. Receiver angular aperture (in milliradians) and cZ, the number of attenuation lengths is also shown.

Although the improvement in contrast achievable with the PG-LLS over the CW-LLS was apparent from the images and computed contrast plots, it is also useful to examine how the image noise levels vary between imaging methods as turbidity increases. Figure 7 shows contrast signal-to-noise ratio (CSNR) (equation 3) for the WoB target. Figure 8 shows CSNR for the BoW target. The initial difference in CSNR between the two imaging methods (from clear water up to 5.5 beam attenuation lengths) is likely due to the imperfect energy normalization of the high pulse-to-pulse energy instability characteristic of the laser being used. However, the PG-LLS method produces lower noise images beyond 5.5 attenuation lengths for both the light and dark background targets. Between 6.1 and 7.6 attenuation lengths the narrow receiver aperture PG-LLS configuration produces lower noise images for both targets, suggesting less forward scattered light entering the receiver.

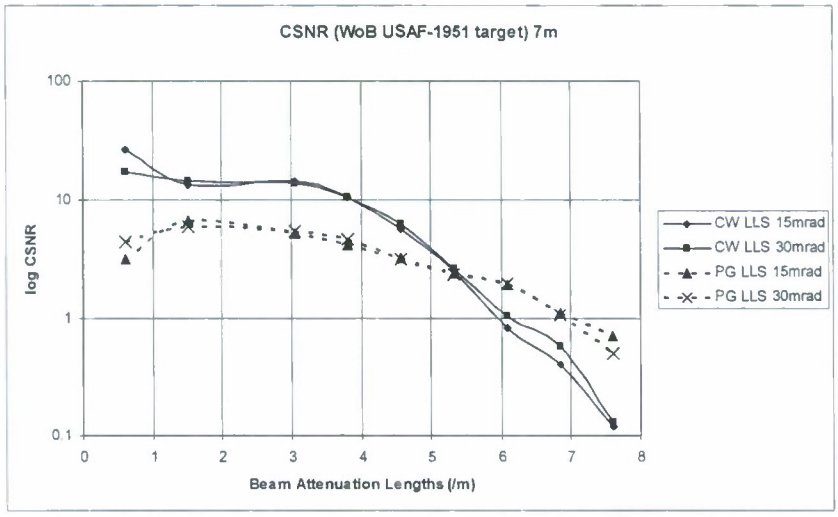

Figure 7: Computed image CSNR for USAF-1951 White-on-Black target at 7m for CW-LLS versus PG-LLS

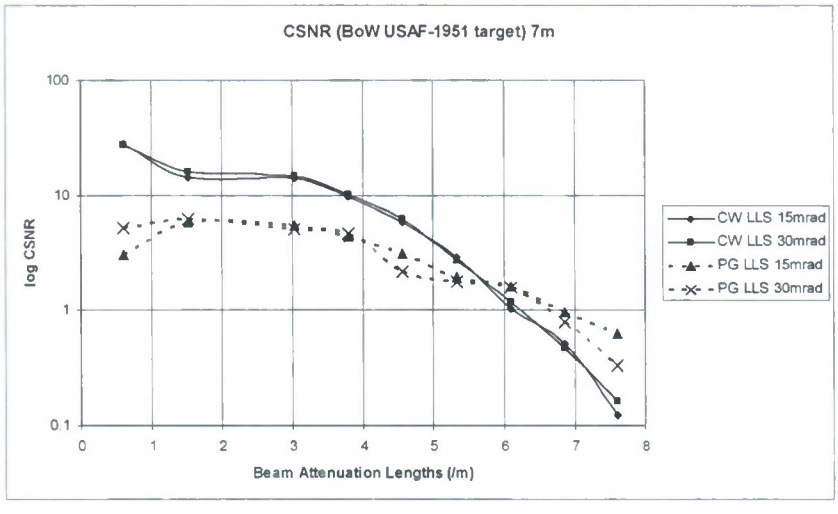

Figure 8: Computed image CSNR for USAF-1951 Black-on-White target at 7m for CW-LLS versus PG-LLS

4. Validation of image simulation code

For both the benchtop CW-LLS and PG-LLS imagers, a set of images were taken at 7 meters stand-off distance. All system, environmental, target and operational parameters were precisely measured and simulated images were produced using the Metron radiative transfer image simulation software. The results for the CW-LLS experimental and analytic cases are shown in figure 9. The final version of the simulation code also included a shot noise model for the PMT. The agreement is excellent across the entire range of attenuation lengths. Similar comparisons are shown for a PG-LLS imager in figure 10, where time gating was used to mitigate the laser backscatter return, both in simulation and experiment. A journal article describing in-depth analysis involved in the validation effort is currently in preparation, but in general the agreement is excellent and demonstrates that the modeling approach can be used as a predictive tool.

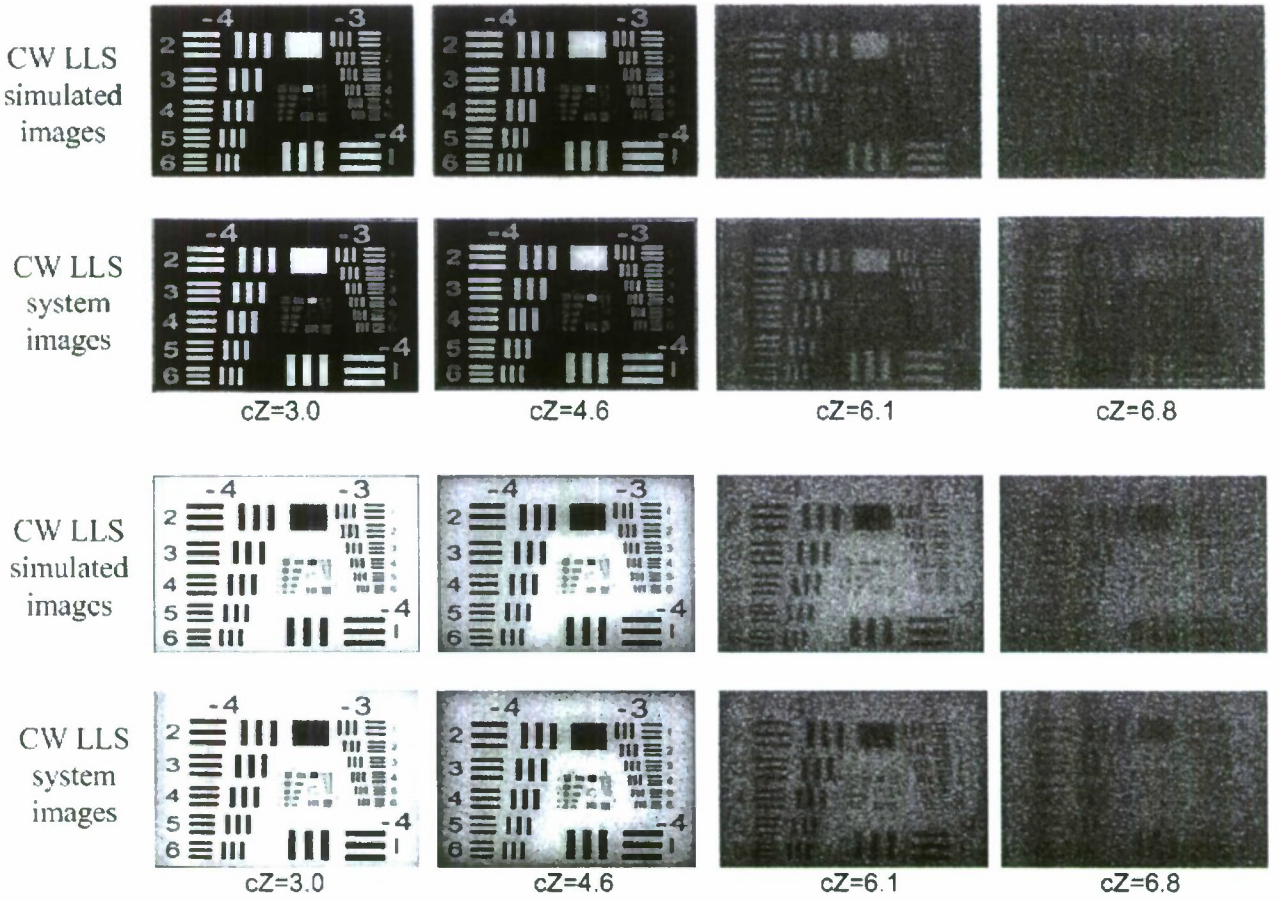

Figure 9: CW-LLS test tank system images versus CW-LLS simulated images at 7 meters. Rows 1 and 3 show the simulated images for each case. Rows 2 and 4 show the benchtop system images. cZ = number of attenuation lengths at 532nm, where c is the attenuation coefficient and Z is the distance to the target.

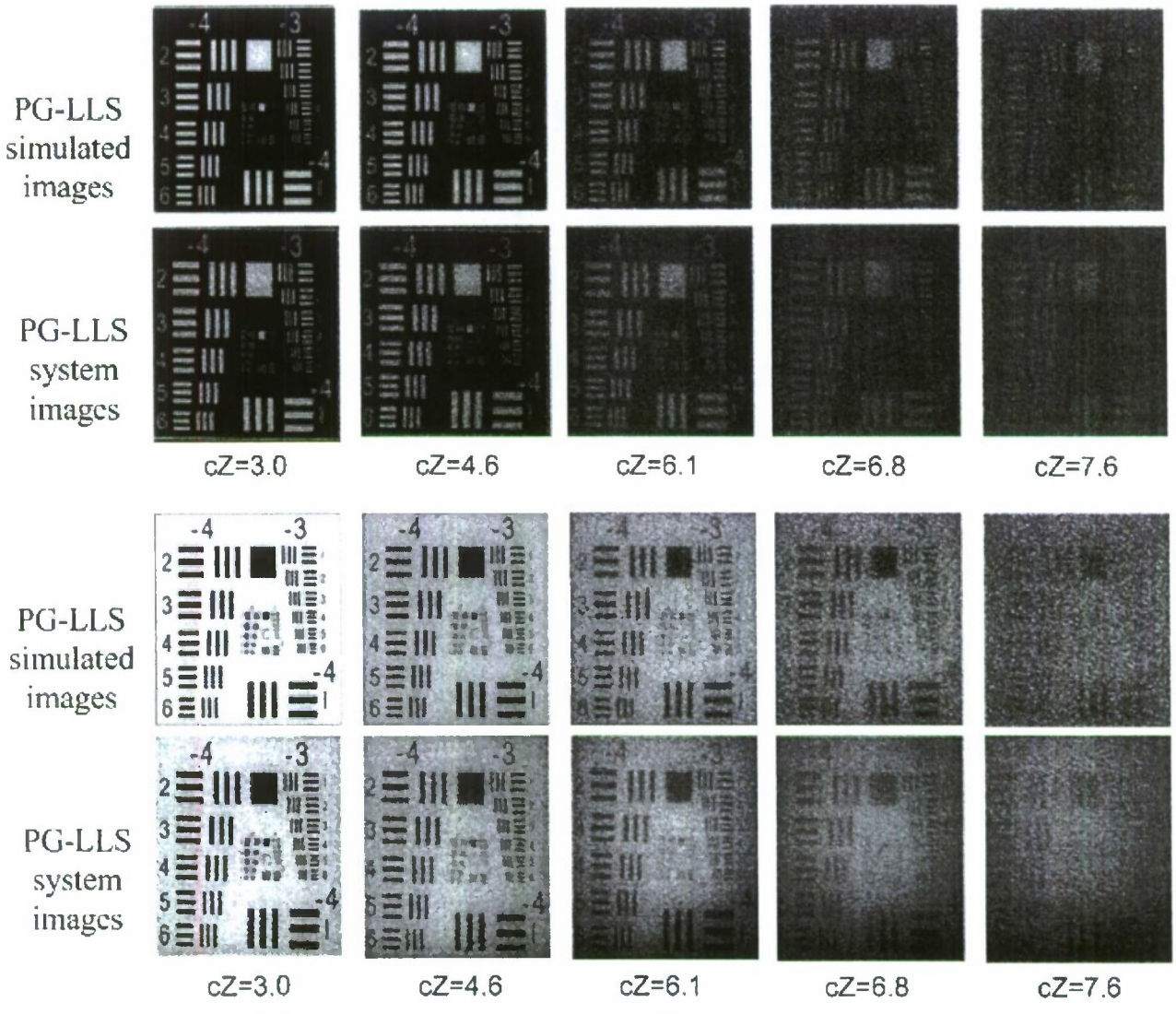

Figure 10: PG-LLS test tank system images versus PG-LLS simulated images at 7 meters. Rows 1 and 3 show the simulated images for each case. Rows 2 and 4 show the benchtop system images. cZ = number of attenuation lengths at 532nm, where c is the attenuation coefficient and Z is the distance to the target.

5. Advanced simulations and experimental validation for modulated-pulses.

Utilizing a finer time resolution version of the pulse time history code, it was possible to investigate the benefits of several alternative modulated-pulse coding schemes. These techniques show potential to reduce forward scatter levels and therefore make improvements in achievable signal-to-noise ratio and timing resolution by careful selection of modulation code and suitable coherent processing algorithm. To produce experimental results supporting this study, a 500ps (40μJ per pulse) green laser was used with a series of beam splitters and mirrors with appropriate delay times to generate a 1GHz amplitude modulation tone. Experiments were conducted through greater than 11 meters of turbid water to compare with simulations results. An additional processing stage was implemented to investigate the enhanced detection of the modulated-pulse using IQ demodulation techniques. A comparison of the

Metron model output versus measured data for the modulated-pulse case is shown on the top plot of each graphset in figure 11. Aside from system noise and difficulties in producing perfect laser waveforms for the experiments, the conformance appears to be satisfactory. IQ demodulation results (from top to bottom for each plot: raw signal, low pass filter I, I, low pass filtered Q, Q, phase and magnitude) are also shown for simulated and measured cases in figure 11. Please note the system delay in the processed results for both cases has not been removed.

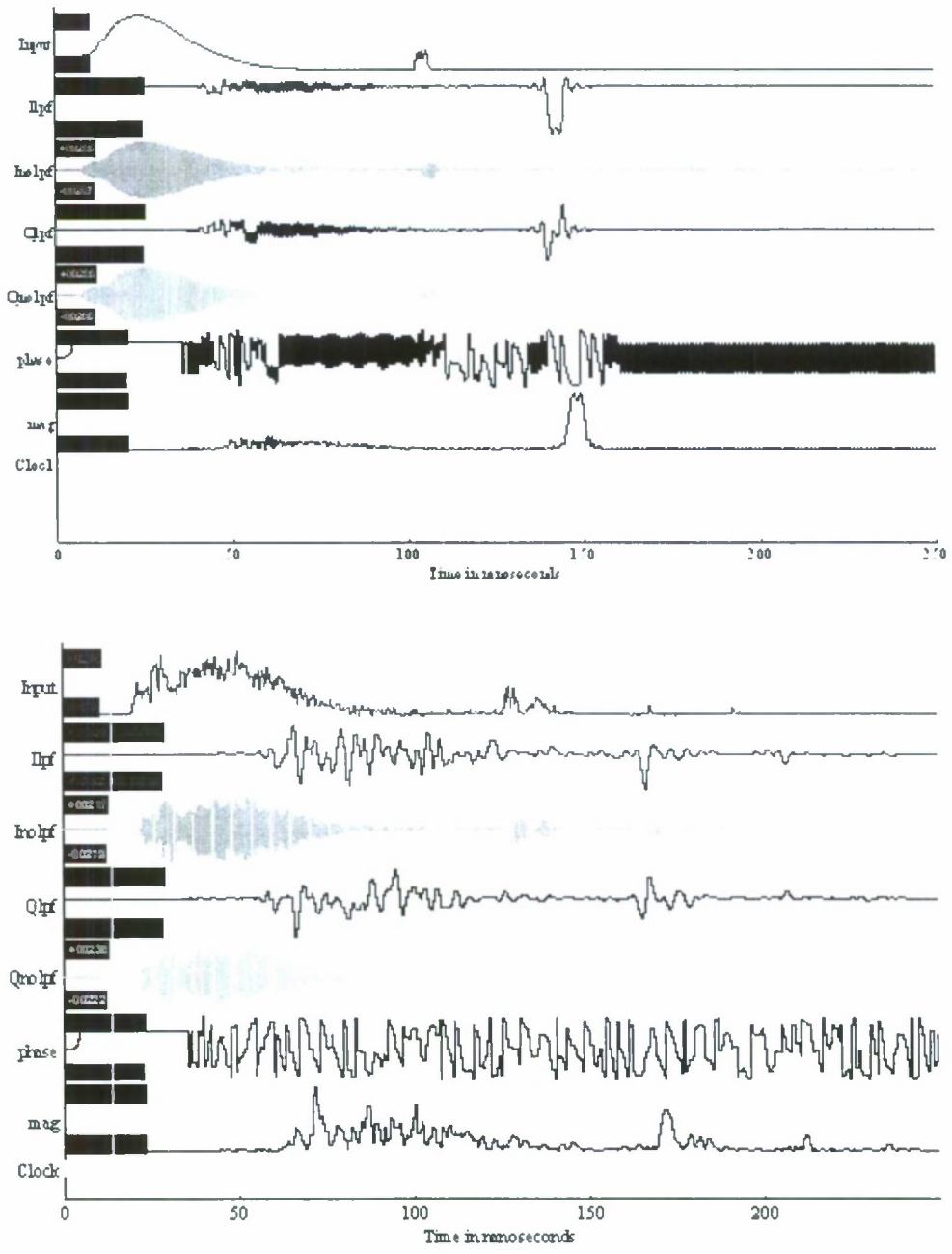

Figure 11: <u>Top graphset:</u> Simulation results with Metron time history code and IQ demodulation processing for a 1GHz modulated pulse with 99% target 11.42m distant (c=0.58m^{-1}, cZ=6.62). <u>Bottom graphset:</u> Experimental results from same case.

IMPACT/APPLICATIONS

The analytic and experimental results demonstrate that the PG-LLS imager is capable of improving image contrast and contrast signal-to-noise ratio (CSNR) in scattering-dominant waters over that of the existing CW-LLS architecture. Results indicate that for the laser-receiver separation of 23.4cm being investigated with the prototype, the PG-LLS imager becomes limited by forward scattered light at > 7 attenuation lengths instead of reaching a contrast limit due to multiple backscatter and shot noise at around 6 attenuation lengths, such as in the case of the CW-LLS. Increased laser pulse energy and stability, improvements in gated receiver performance, together the use of processing to isolate acquired pulses from system noise and the tail end of the backscatter signal may further improve performance. Other possibilities involve using laser sources capable of adding modulation to the laser pulse and the use of coherent processing to reject the forward scatter signal mixed within the main pulse envelope, and this is the subject of ongoing work with collaborators.

The PG-LLS does not require a significant source-receiver separation to produce quality images, and hence allows for more compact, simpler optical designs suitable for smaller operational plaforms and having the potential to be more immune to changes in operating conditions, hence more reliable than the current state-of-the-art. Future advances in pulsed laser source technology should allow for these imagers soon to be packaged suitably small for modern unmanned underwater platforms such as the man-portable autonomous underwater vehicles.

Technical developments and validation experiments conducted under Advanced Underwater Imaging (AUI) program have been key factors in the development, validation, and certification of EODES models. EODES image simulation and performance prediction models for underwater electro-optical systems are part of a long-standing research and development project supported by the Office of Naval Research (ONR). EODES simulation tools are currently being used to support the development of next-generation electro-optical identification (EOID) systems and the EODES performance prediction models are currently being incorporated into near real-time Navy tactical decision aids, which have been successfully demonstrated by the Naval Oceanographic Office (NAVOCEANO) during RIMPAC exercises in 2006 and 2008. These EODES models are currently undergoing evaluation for inclusion in the Oceanographic and Atmospheric Master Library (OAML) and a technology transition to NAVOCEANO. Ongoing model enhancements have the overall aim of adapting the previously developed and validated EODES computer model to allow the user to exercise a greater degree of spatial and angular disparity between the source and the receiver, to allow accurate and efficient simulation for a distributed LLS imaging and communications concept, which in future scenarios could involve deploying multiple laser illuminators and receivers on multiple underwater vehicles.

RELATED PROJECTS

A Navair SBIR phase II is being performed in collaboration with Advanced Technologies Group (Stuart, FL) to develop a high performance Gated Lidar-radar demodulating receiver for underwater LLS imagers.

HBOI Underwater Laser Imaging and Communications Research – Phase I. ONR-monitored applied research (FY09). This project will adapt the EODES model for the distributed LLS concept. Test-tank demonstration and experimental validation will be performed as part of this work.

PUBLICATIONS

Dalgleish, F. R., Caimi, F. M., Britton, W. B., and Andren, C. F. 2009. "Experimental Comparison of CW and pulse-gated synchronous scanning underwater imagers in scatter-dominant waters," *In preparation for SPIE Optical Engineering.*

Dalgleish, F. R., Caimi, F. M., Britton, W. B., Giddings T.E., Shirron, J.J. and Mazel, C. H. 2009. "Experimental validation of an underwater electro-optical image prediction tool," *In preparation for Applied Optics.*

Dalgleish, F. R. Caimi, F. M. Britton W. B. and Andren C. F. 2009 "Improved LLS imaging performance in scattering-dominant waters," *Proceedings of SPIE, Vol. 7317, (2009).*

Dalgleish, F. R., Caimi, F. M., Britton, W. B., Andren C. F. and Wan Y. 2008. "Experimental comparison of pulsed-gated and continuous wave LLS underwater imagers," *Ocean Optics XIX. October 6-10 2008, Barga, Italy.*

Dalgleish, F. R., Caimi, F. M., Britton, W. B., Wan, Y., Mazel, C. H., Glynn, J. M., Towle, J. P., Giddings T. and Shirron, J. 2008. "Experimental validation of a laser pulse time history model," *Ocean Optics XIX. October 6-10 2008, Barga, Italy.*

Caimi, F. M., Dalgleish, F. R., Kocak, D. M., and Watson, J. 2008. "Underwater Optics and Imaging: Recent Advances," *Oceans 2008, September 15-18 2008, Quebec City, Canada.*

Kocak, D. M., Dalgleish, F. R., Caimi, F. M., and Schechner, Y. Y. "A Focus on Recent Developments and Trends in Underwater Imaging," *MTS Journal, Spring 2008, 42(1):50-65.*

Dalgleish, F. R., Caimi, F. M., Britton, W. B. and Andren, C. F., "An AUV-deployable pulsed laser line scan (PLLS) imaging sensor," *Oceans 2007, October 2-5, Vancouver, Canada.*

Caimi, F. M., Dalgleish, F. R., Giddings, T. E. Shirron, J. J., Mazel, C. H., Chiang, K. "Pulse versus CW laser line scan imaging detection methods: simulation results," *Oceans Europe 2007, June 18-21, 2007, Aberdeen, Scotland.*

Dalgleish, F. R., Caimi, F. M., Mazel, C. H., Glynn, J. M., Chiang, K., Giddings, T. E. and Shirron, J. J. "Model-based evaluation of pulsed lasers for an underwater laser line scan imager," *Ocean Optics XVIII. October 9-11, 2006, Montreal, Canada.*

Dalgleish, F. R., Bordner, P. R and Caimi, F. M. "HBOI extended range optical imaging test facility," *Ocean Optics XVIII. October 9-11, 2006, Montreal, Canada.*

Dalgleish, F. R., Caimi, F. M., Mazel, C. H. and Glynn, J. M. "Extended Range Underwater Optical Imaging Architecture," *MTS/IEEE Oceans 2006, September 18-21 2006, Boston, MA.*

PATENTS

METHOD AND APPARATUS FOR SYNCHRONOUS LASER BEAM SCANNING. U.S. Patent Application No. 11/857,039